

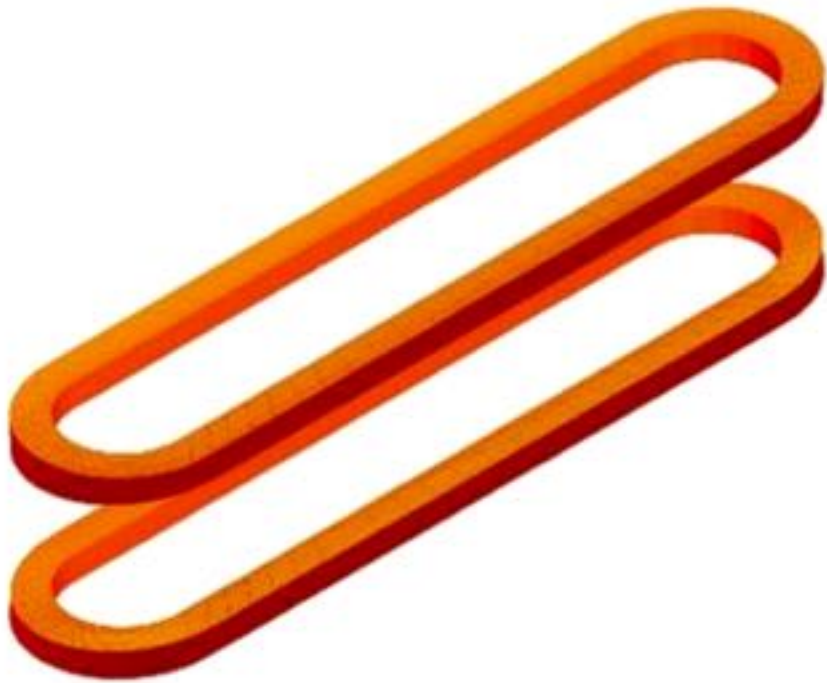
Electromagnetic Design of Accelerator Magnets and ROXIE User's Course

Coil-end design

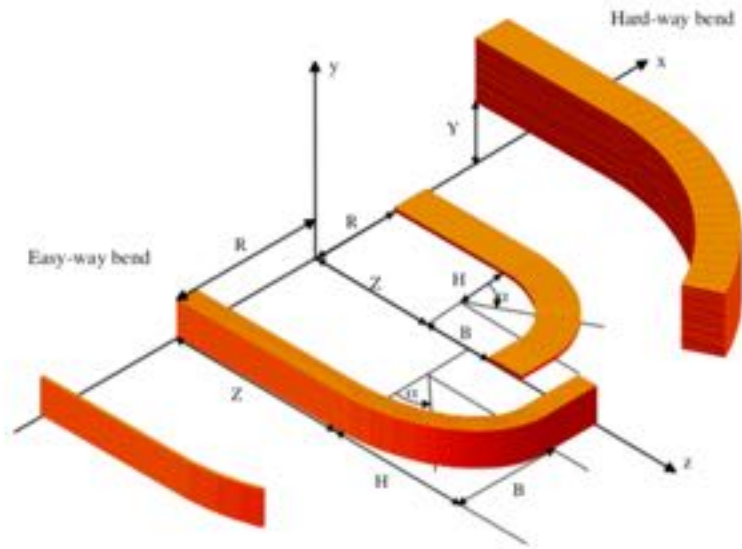
Stephan Russenschuck, CERN, 2022



Racetrack and Constant Perimeter Coils

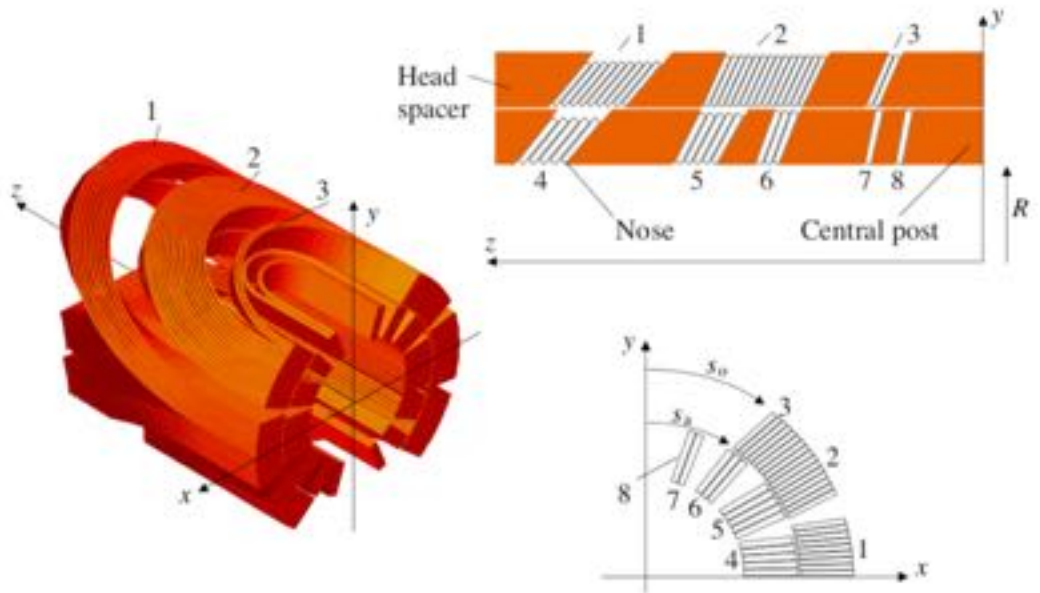


A Few Conventions



Hard-way bend

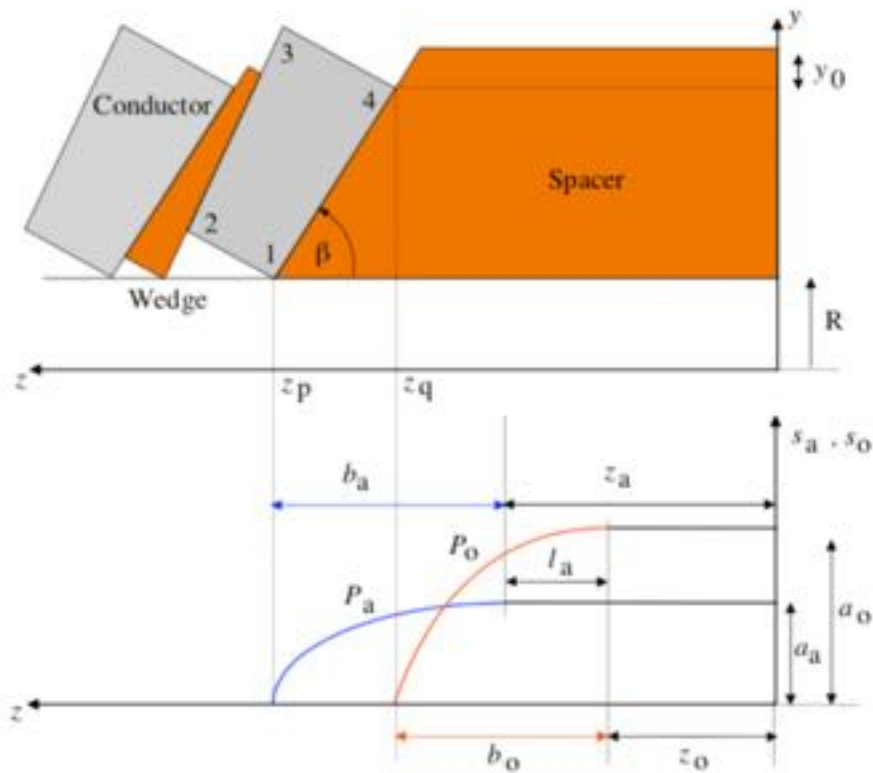
Soft-way bend



Coil and End-spacers



Constant-Perimeter Ends



Perimeter of outer (free) edge

$$P_o = b_o E \left(\frac{\pi}{2}, e \right)$$

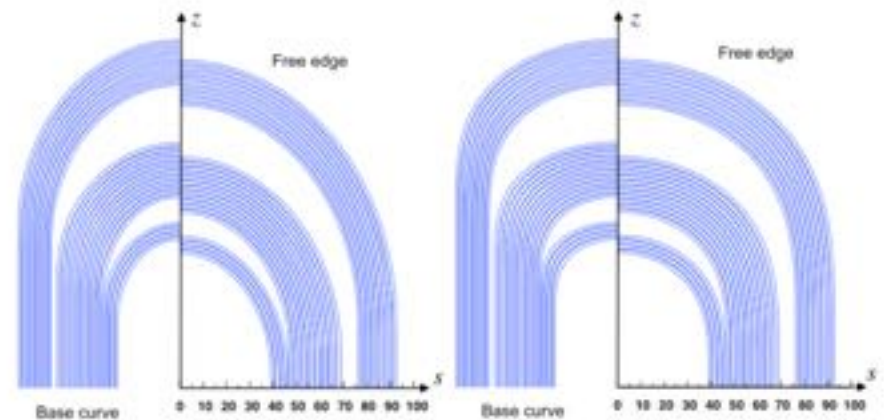
$$e := \sqrt{1 - \frac{a_o^2}{b_o^2}}$$

$$P_o \approx \frac{1}{4} \pi (a_o + b_o) \left(1 + \frac{\lambda^2}{4} + \frac{\lambda^4}{64} \right),$$

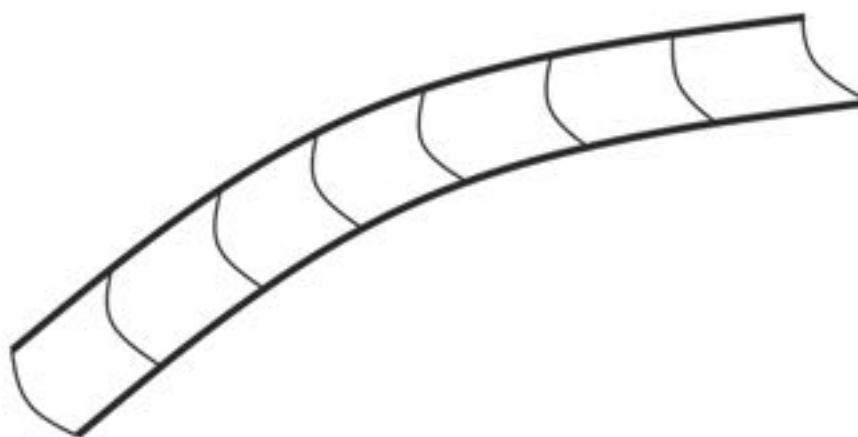
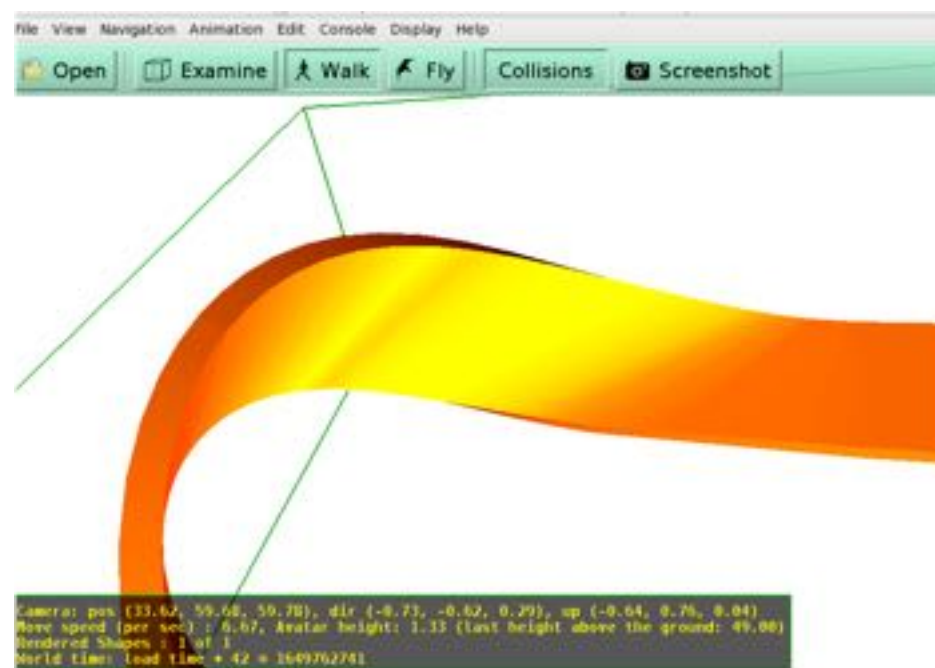
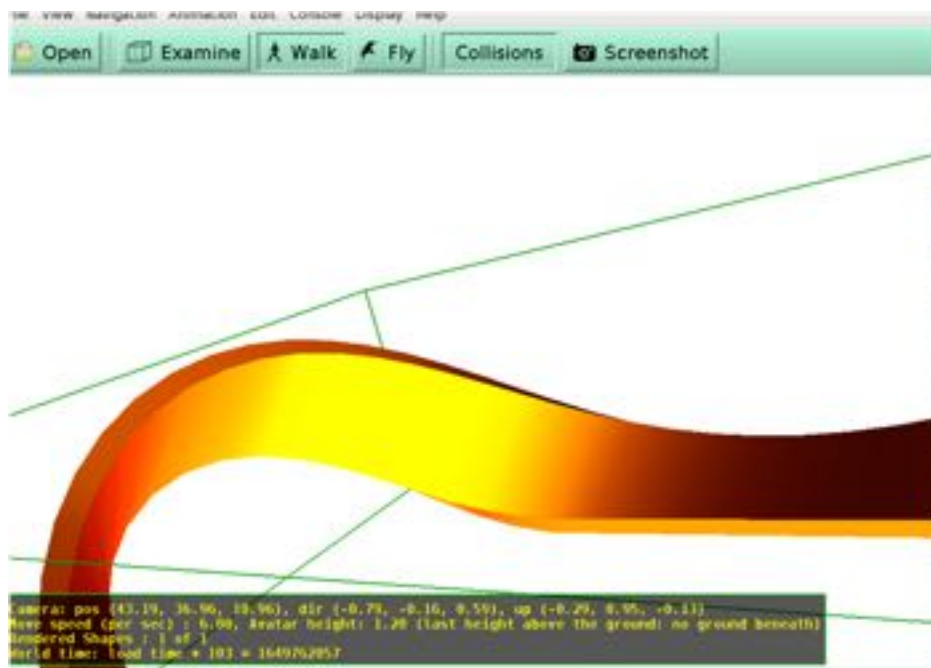
$$\lambda := \frac{a_o - b_o}{a_o + b_o}$$

$$P_a \approx \frac{1}{4} \pi (a_a + b_a) \left(1 + \frac{v^2}{4} + \frac{v^4}{64} \right),$$

$$v := \frac{a_a - b_a}{a_a + b_a}$$



Constant Perimeter Ends are not (Necessarily) Developable



Freney Frame of Space Curves

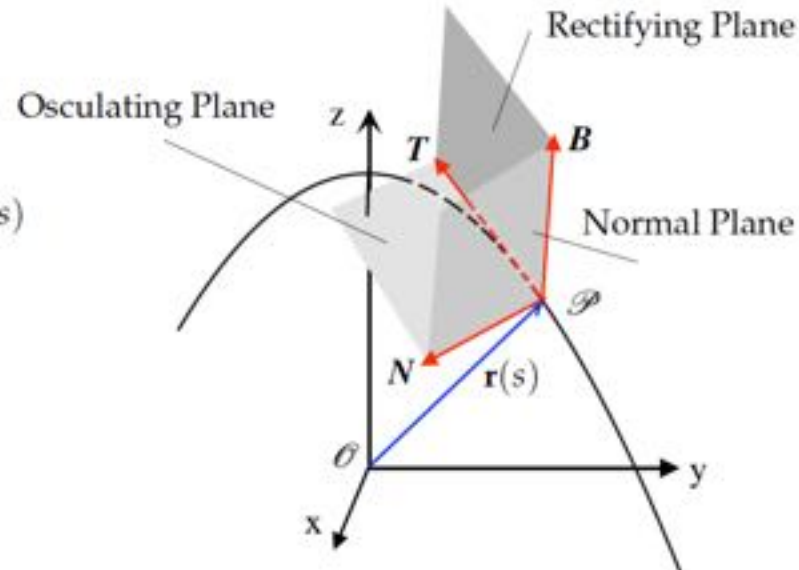
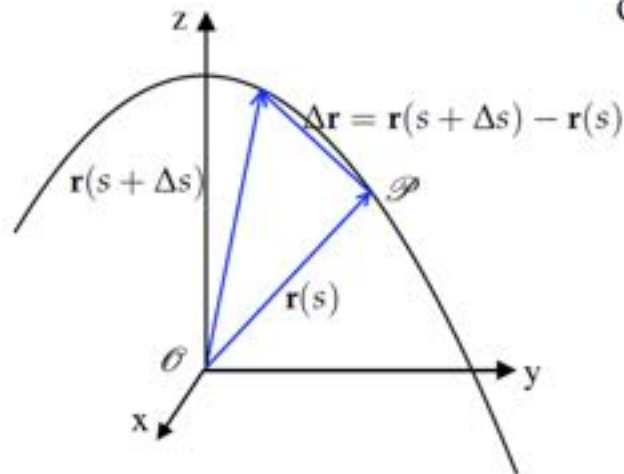
$$\frac{d\mathbf{r}(t)}{dt} = \mathbf{v}(t) = \frac{d}{dt}(r\mathbf{e}_r + z\mathbf{e}_z) = \frac{dr}{dt}\mathbf{e}_r + r\frac{d\mathbf{e}_r}{dt} + \frac{dz}{dt}\mathbf{e}_z + z\frac{d\mathbf{e}_z}{dt},$$

Unit speed

$$\frac{df(s(t))}{dt} = \frac{df}{ds} \frac{ds}{dt} = v \frac{df}{ds}$$

$$\mathbf{T}(t) := \frac{\mathbf{v}(t)}{v(t)} = T_x(t)\mathbf{e}_x + T_y(t)\mathbf{e}_y + T_z(t)\mathbf{e}_z.$$

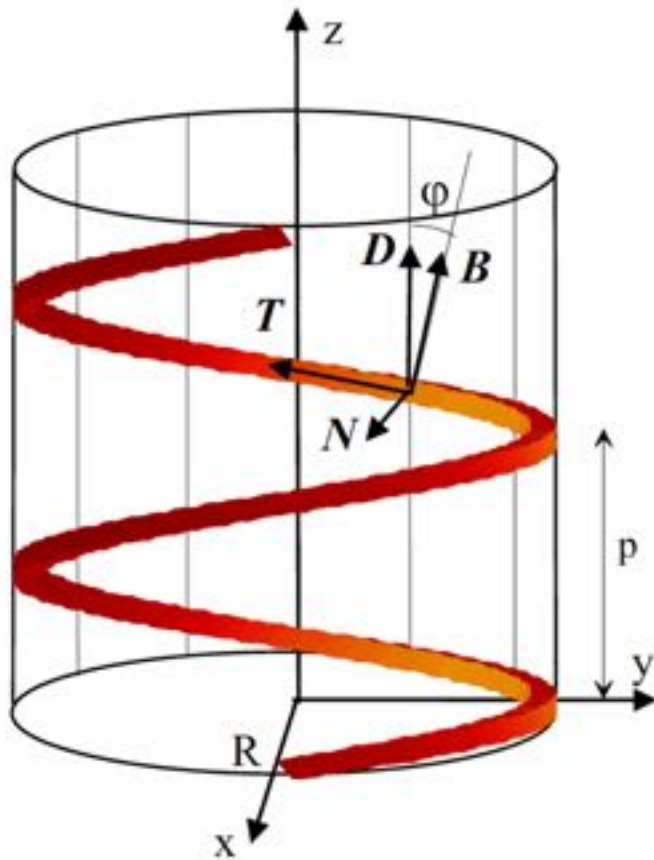
$$\mathbf{T}(s) = \frac{1}{v} \frac{d\mathbf{r}(t)}{dt} = \frac{d\mathbf{r}(s)}{ds}$$



$$\mathbf{T}' = \mathbf{r}'' = |\mathbf{T}'| \mathbf{N} =: \kappa \mathbf{N},$$

$$\mathbf{B} = \mathbf{T} \times \mathbf{N}$$

The Helix and the Darboux Vector



$$\mathbf{D} = \tau \mathbf{T} + \kappa \mathbf{B} = \frac{1}{\sqrt{R^2 + q^2}} \mathbf{e}_z.$$

Axis of rotation of the Frenet frame

Frenet frame

$$\mathbf{T}' = \kappa \mathbf{N},$$

$$\mathbf{N}' = \tau \mathbf{B} - \kappa \mathbf{T},$$

$$\mathbf{B}' = -\tau \mathbf{N}$$

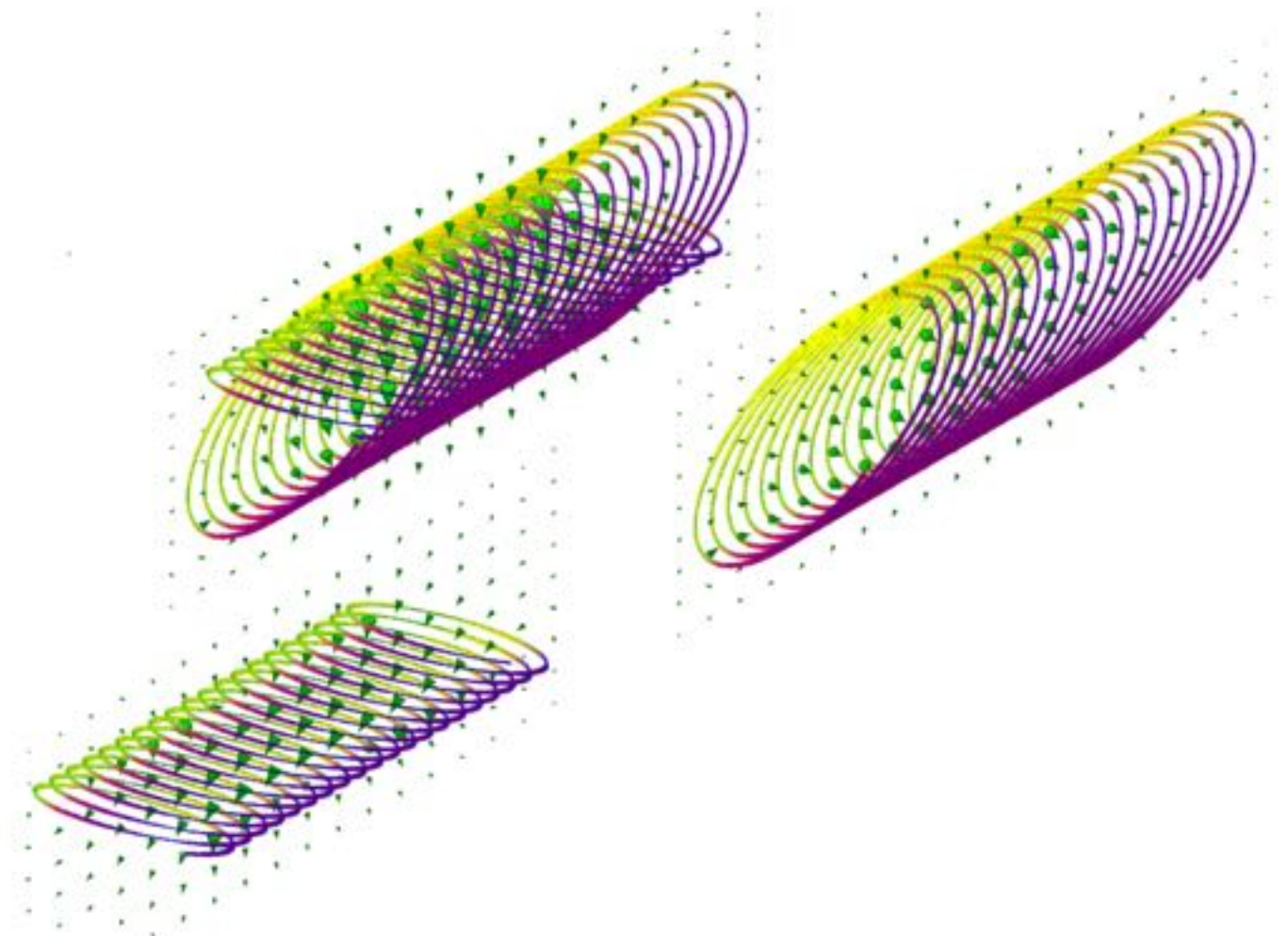
$$\mathbf{T}' = \mathbf{D} \times \mathbf{T},$$

$$\mathbf{N}' = \mathbf{D} \times \mathbf{N},$$

$$\mathbf{B}' = \mathbf{D} \times \mathbf{B}$$

The CCT Magnet Concept

CCT is a better term than titled helix because the quotient of torsion to curvature is not constant



The Space Curve and the Frenet Frame

$$\mathbf{r}(\varphi) = R \cos(\varphi) \mathbf{e}_x + R \sin(\varphi) \mathbf{e}_y + s(\varphi) \mathbf{e}_z,$$

with

$$s(\varphi) = R \tan(\alpha) \sin(n\varphi) + p \frac{\varphi}{2\pi}.$$

$$\mathbf{r} = R \mathbf{e}_r + s(\varphi) \mathbf{e}_z = R \mathbf{e}_r + \left(R \tan(\alpha) \sin(n\varphi) + \frac{p}{2\pi} \varphi \right) \mathbf{e}_z,$$

$$\mathbf{v} = R \mathbf{e}_\varphi + s'(\varphi) \mathbf{e}_z = R \mathbf{e}_\varphi + \left(nR \tan(\alpha) \cos(n\varphi) + \frac{p}{2\pi} \right) \mathbf{e}_z,$$

$$\mathbf{a} = -R \mathbf{e}_r + s''(\varphi) \mathbf{e}_z = -R \mathbf{e}_r - n^2 R \tan(\alpha) \sin(n\varphi) \mathbf{e}_z,$$

$$\mathbf{a}' = -R \mathbf{e}_\varphi + s'''(\varphi) \mathbf{e}_z = -R \mathbf{e}_\varphi - n^3 R \tan(\alpha) \cos(n\varphi) \mathbf{e}_z,$$

$$\mathbf{v} \times \mathbf{a} = R s''(\varphi) \mathbf{e}_r - R s'(\varphi) \mathbf{e}_\varphi + R^2 \mathbf{e}_z.$$



The Space Curve and the Frenet Frame

$$\mathbf{r}(\varphi) = R \cos(\varphi) \mathbf{e}_x + R \sin(\varphi) \mathbf{e}_y + s(\varphi) \mathbf{e}_z,$$

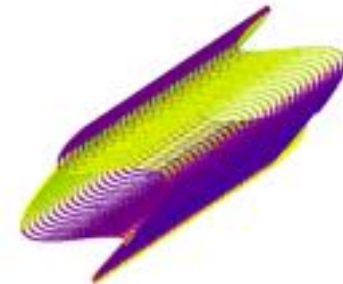
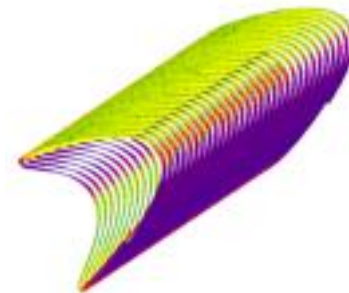
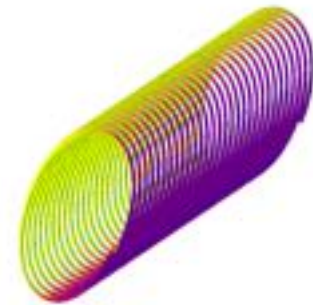
with

$$s(\varphi) = R \tan(\alpha) \sin(n\varphi) + p \frac{\varphi}{2\pi}.$$

$$\mathbf{T} = \frac{R \mathbf{e}_\varphi + s'(\varphi) \mathbf{e}_z}{\sqrt{R^2 + (s'(\varphi))^2}},$$

$$\mathbf{B} = \frac{Rs''(\varphi) \mathbf{e}_r - Rs'(\varphi) \mathbf{e}_\varphi + R^2 \mathbf{e}_z}{\sqrt{(Rs''(\varphi))^2 + (Rs'(\varphi))^2 + R^4}},$$

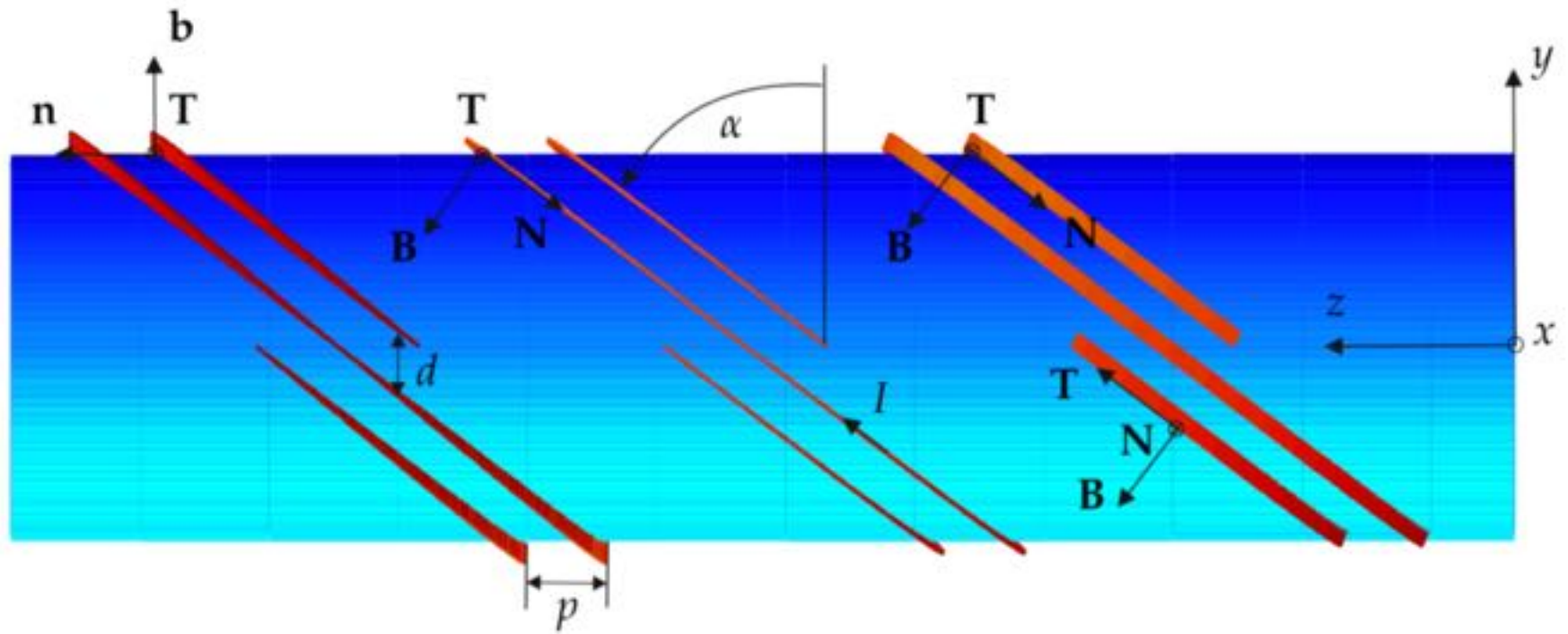
$$\mathbf{N} = \frac{-R(s'(\varphi))^2 - R^3 \mathbf{e}_r - Rs''(\varphi) s'(\varphi) \mathbf{e}_\varphi + R^2 s''(\varphi) \mathbf{e}_z}{\sqrt{(R^2 + (s'(\varphi))^2) (Rs''(\varphi))^2 + (Rs'(\varphi))^2 + R^4}}.$$



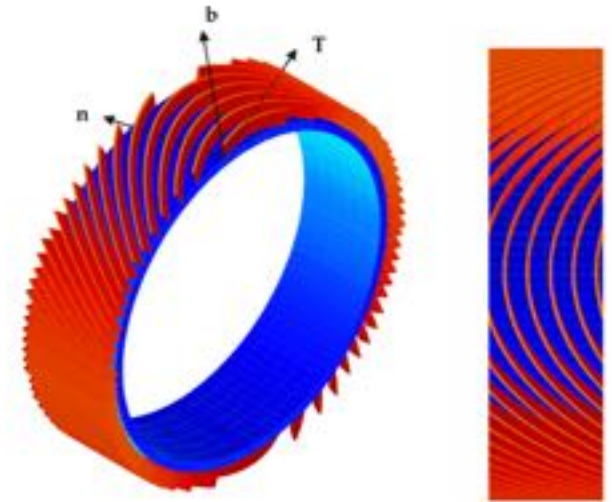
Darboux

Frenet (hard-way)

Frenet (soft-way)



The Darboux Frame



Darboux

Frenet

$$\begin{pmatrix} \mathbf{T} \\ \mathbf{n} \\ \mathbf{b} \end{pmatrix} = \begin{pmatrix} 1 & 0 & 0 \\ 0 & \cos(\vartheta_{\mathbf{T}}) & -\sin(\vartheta_{\mathbf{T}}) \\ 0 & \sin(\vartheta_{\mathbf{T}}) & \cos(\vartheta_{\mathbf{T}}) \end{pmatrix} \begin{pmatrix} \mathbf{T} \\ \mathbf{N} \\ \mathbf{B} \end{pmatrix}$$

$$\tau = \tau + \frac{1}{|\mathbf{v}|} \frac{d\vartheta_{\mathbf{T}}}{d\varphi_c}, \quad \kappa_g = \kappa \cos(\vartheta_{\mathbf{T}}), \quad \kappa_n = \kappa \sin(\vartheta_{\mathbf{T}})$$

$$\mathbf{T} = \frac{R \mathbf{e}_\varphi + s'(\varphi) \mathbf{e}_z}{\sqrt{R^2 + (s'(\varphi))^2}}$$

$$\mathbf{b} = \mathbf{e}_r,$$

$$\mathbf{n} = -\mathbf{T} \times \mathbf{e}_r = \frac{-s'(\varphi) \mathbf{e}_\varphi + R \mathbf{e}_z}{\sqrt{R^2 + (s'(\varphi))^2}}.$$

The assumption makes the mathematics easy, but also life?

Some hand-waving arguments

$$d = |p \mathbf{e}_z \cdot \mathbf{n}| = \frac{Rp}{\sqrt{R^2 + (s'(\varphi_c))^2}} = \frac{Rp}{|\mathbf{v}|}$$



$$B_1 = \frac{\mu_0 I_0}{2r_c p} \tan(\alpha)$$

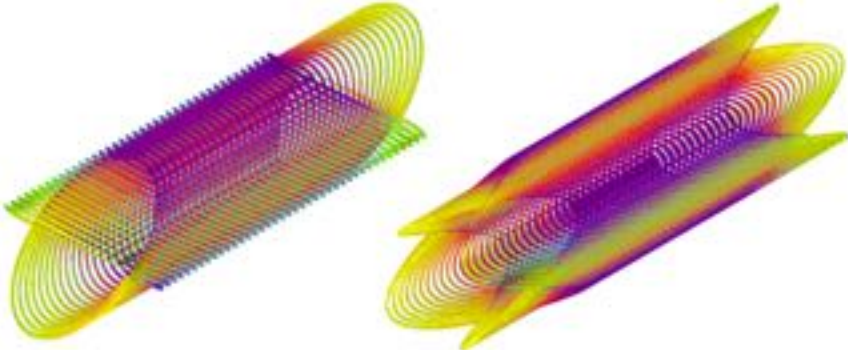
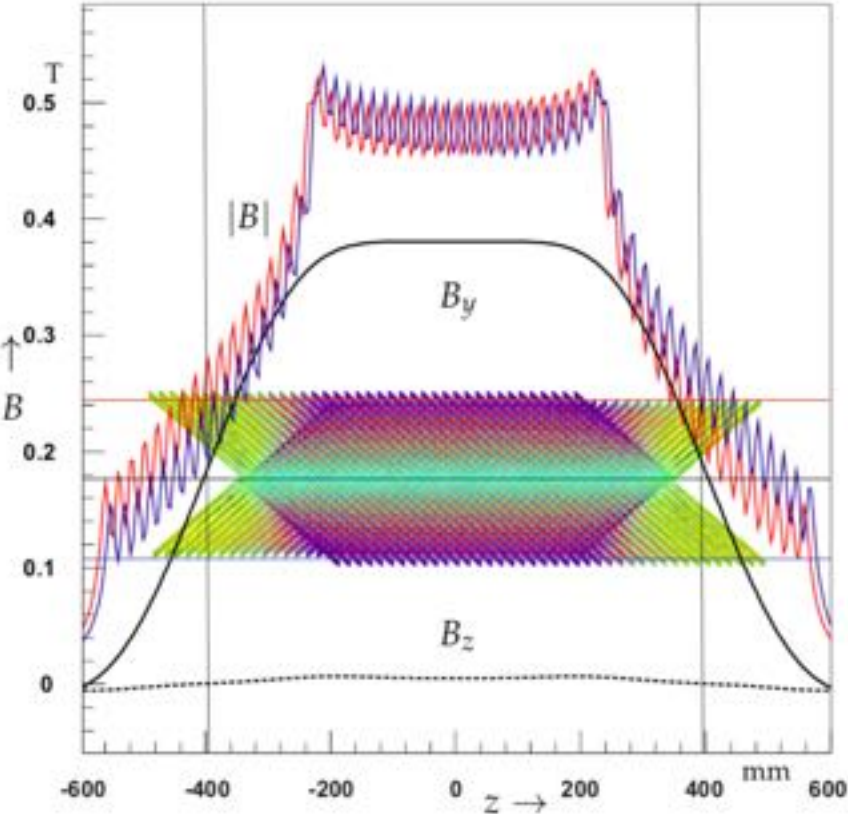
Pitch-averaged surface current

$$\boldsymbol{\alpha}(\varphi_c) = \frac{I_0 \mathbf{T}}{d} = \frac{I_0}{Rp} \mathbf{v}$$

$$B_z(0,0) = \frac{\mu_0 I_0}{p}$$

$$\mathbf{v} = R \mathbf{e}_\varphi + s'(\varphi_c) \mathbf{e}_z = R \mathbf{e}_\varphi + \left(nR \tan(\alpha) \cos(n\varphi_c) + \frac{p}{2\pi} \right) \mathbf{e}_z,$$

Local Field Enhancements



Curved CCT

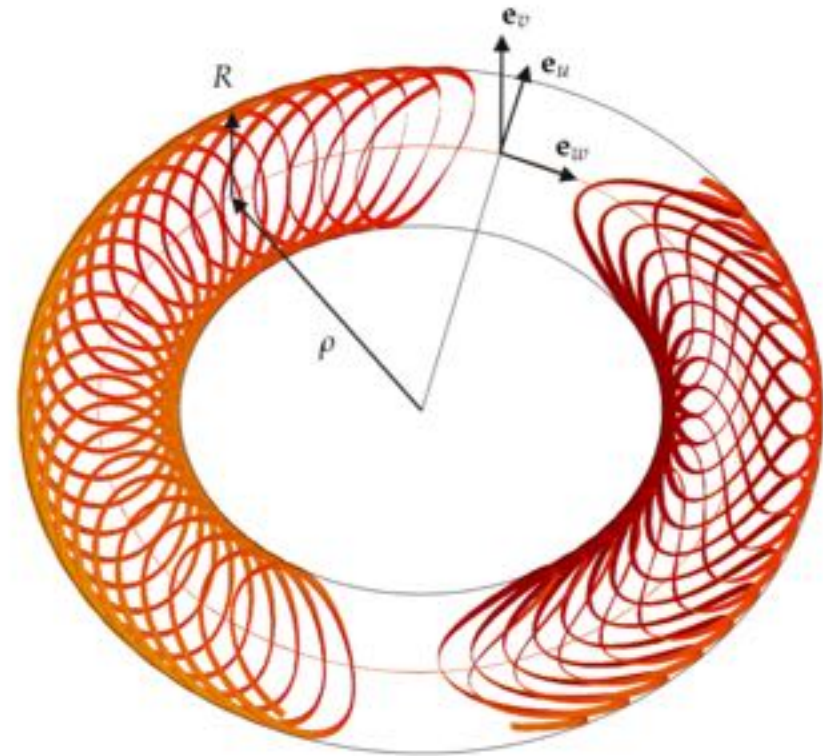
$$\mathbf{o}(s) = \rho \cos\left(\frac{s}{\rho}\right) \mathbf{e}_x + \rho \sin\left(\frac{s}{\rho}\right) \mathbf{e}_z$$

$$s(\varphi) = R \tan(\alpha) \sin(n\varphi) + p \frac{\varphi}{2\pi}$$

$$\mathbf{e}_u = \cos\left(\frac{s}{\rho}\right) \mathbf{e}_x + \sin\left(\frac{s}{\rho}\right) \mathbf{e}_z,$$

$$\mathbf{e}_v = \mathbf{e}_y,$$

$$\mathbf{e}_w = -\sin\left(\frac{s}{\rho}\right) \mathbf{e}_x + \cos\left(\frac{s}{\rho}\right) \mathbf{e}_z.$$



$$\begin{aligned} \mathbf{r}(\varphi) &= \mathbf{o}(s(\varphi)) + R \cos(\varphi) \mathbf{e}_u(s(\varphi)) + R \sin(\varphi) \mathbf{e}_v(s(\varphi)) \\ &= \cos\left(\frac{s(\varphi)}{\rho}\right) (\rho + R \cos(\varphi)) \mathbf{e}_x + R \sin(\varphi) \mathbf{e}_y \\ &\quad + \sin\left(\frac{s(\varphi)}{\rho}\right) (\rho + R \cos(\varphi)) \mathbf{e}_z. \end{aligned}$$

The Darboux Frame of Curved CCTs

$$\mathbf{T} = \frac{v_x \mathbf{e}_x + v_y \mathbf{e}_y + v_z \mathbf{e}_z}{\sqrt{v_x^2 + v_y^2 + v_z^2}}$$

$$v_x(\varphi) = \frac{1}{\rho} \left(-R\rho \sin(\varphi) \cos\left(\frac{s(\varphi)}{\rho}\right) - (R \cos(\varphi) + \rho) \sin\left(\frac{s(\varphi)}{\rho}\right) s'(\varphi) \right),$$

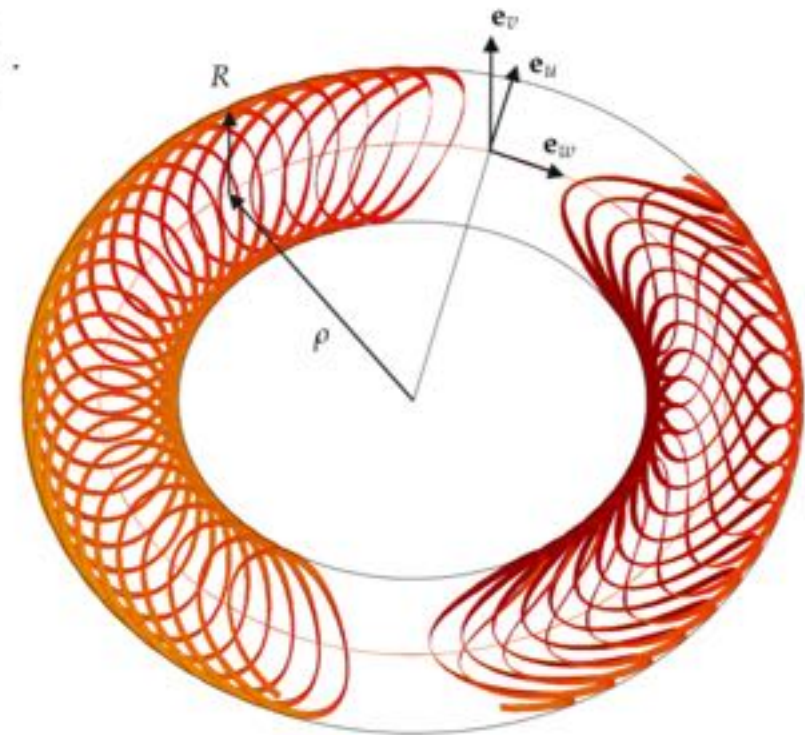
$$v_y(\varphi) = R \cos(\varphi),$$

$$v_z(\varphi) = \frac{1}{\rho} \left(-R\rho \sin(\varphi) \sin\left(\frac{s(\varphi)}{\rho}\right) + (R \cos(\varphi) + \rho) \cos\left(\frac{s(\varphi)}{\rho}\right) s'(\varphi) \right).$$

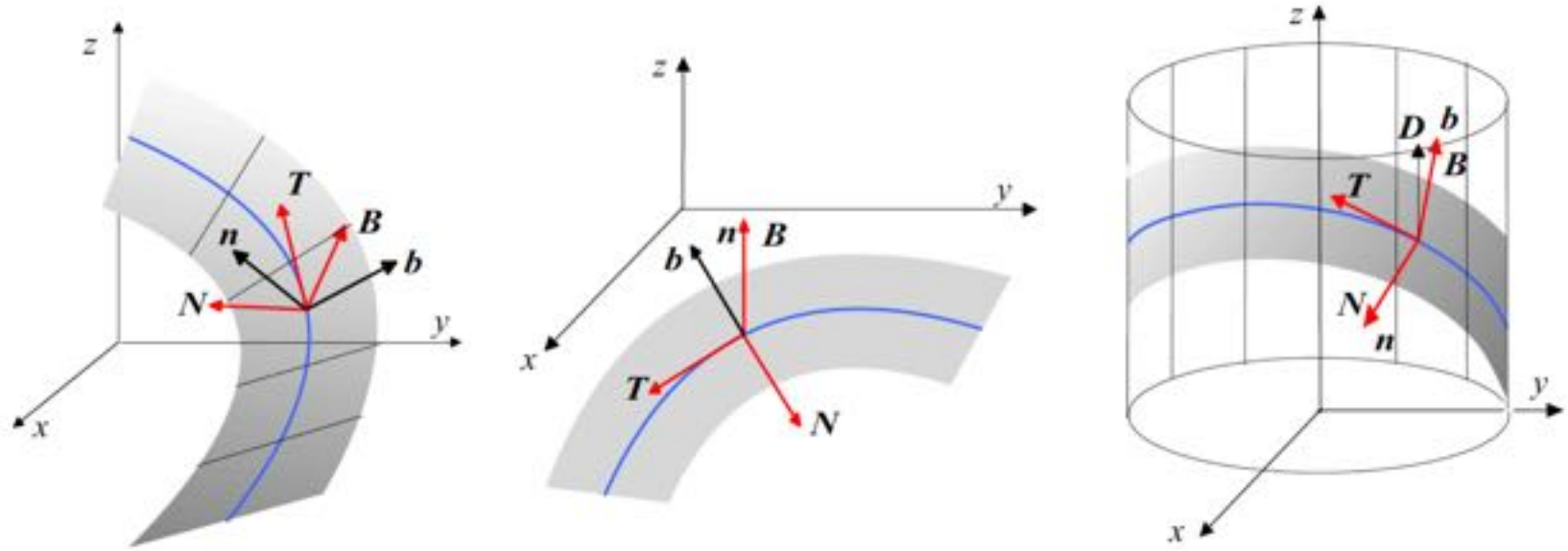
$$\mathbf{b}(\varphi) = \cos(\varphi) \mathbf{e}_u(s(\varphi)) + \sin(\varphi) \mathbf{e}_v(s(\varphi))$$

$$= \cos(\varphi) \cos\left(\frac{s(\varphi)}{\rho}\right) \mathbf{e}_x + \sin(\varphi) \mathbf{e}_y + \cos(\varphi) \sin\left(\frac{s(\varphi)}{\rho}\right) \mathbf{e}_z.$$

$$\mathbf{n} = -\mathbf{T} \times \mathbf{b}.$$



Geodesic Strips



$$\begin{pmatrix} \mathbf{T}' \\ \mathbf{n}' \\ \mathbf{b}' \end{pmatrix} = \begin{pmatrix} 0 & \kappa_n & -\kappa_g \\ -\kappa_n & 0 & \tau \\ \kappa_g & -\tau & 0 \end{pmatrix} \begin{pmatrix} \mathbf{T} \\ \mathbf{n} \\ \mathbf{b} \end{pmatrix}$$

$$\begin{pmatrix} \mathbf{T}' \\ \mathbf{N}' \\ \mathbf{B}' \end{pmatrix} = \begin{pmatrix} 0 & \kappa & 0 \\ -\kappa & 0 & \tau \\ 0 & -\tau & 0 \end{pmatrix} \begin{pmatrix} \mathbf{T} \\ \mathbf{N} \\ \mathbf{B} \end{pmatrix}$$

Limits of the Guiding Strip Theory

- Rutherford cable is not a strip of zero thickness
- Transverse cross-section is keystone
- The cables must be wound onto each other in groups of up to 30 cables
- Inclination in the yz cross-section deviates from the ideal angle
- At the onset, cables lie along a straight line with zero curvature
- Edge of regression may lay inside the strip surface

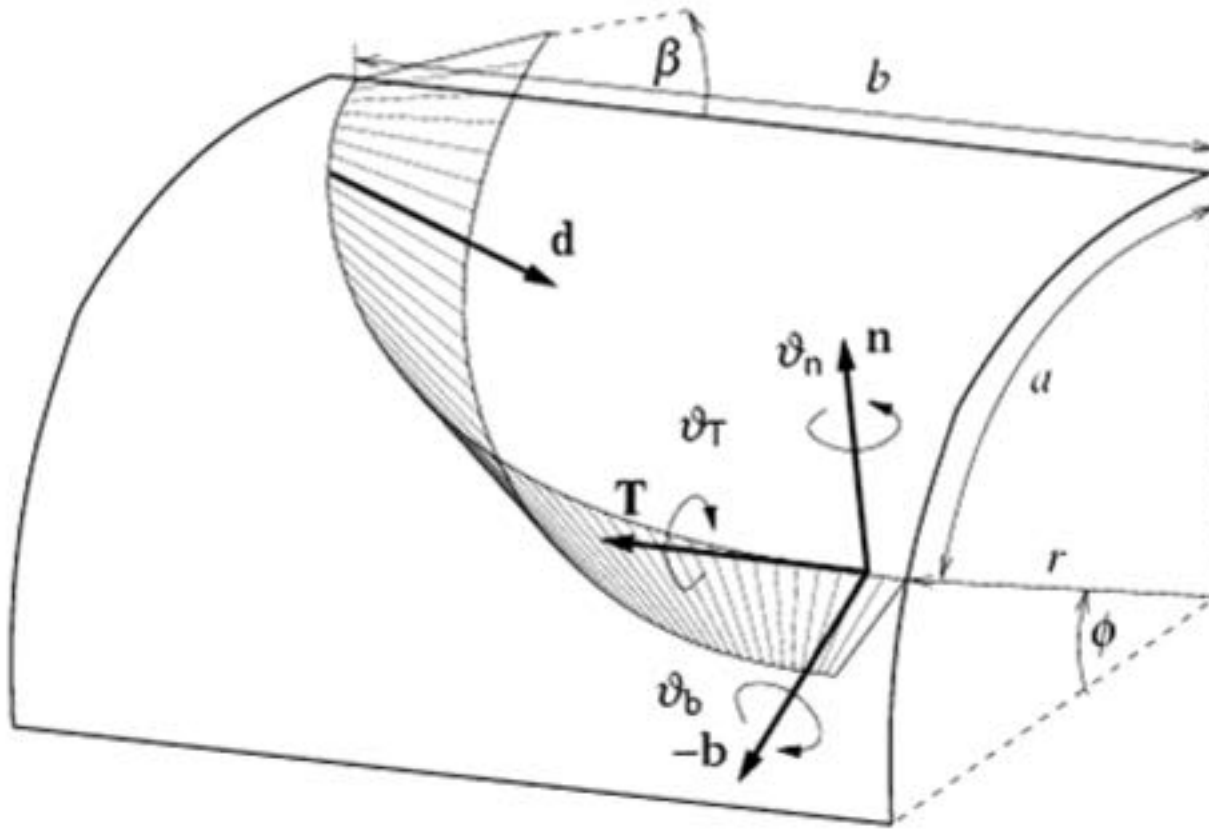
- Minimization of the local hard way deformation through optimal distribution of the twist and optimal order of the hyper-ellipse and the ellipticity ratio

Twist Angles

$$\tau = \bar{b} \cdot \bar{n}' = \vartheta_{\bar{T}'}$$

$$\kappa_g = \bar{T} \cdot \bar{b}' = \vartheta_{\bar{n}'}$$

$$\kappa_n = \bar{n} \cdot \bar{T}' = \vartheta_{\bar{b}'}$$



$$a_a = R\left(\frac{\pi}{2} - \phi\right)$$

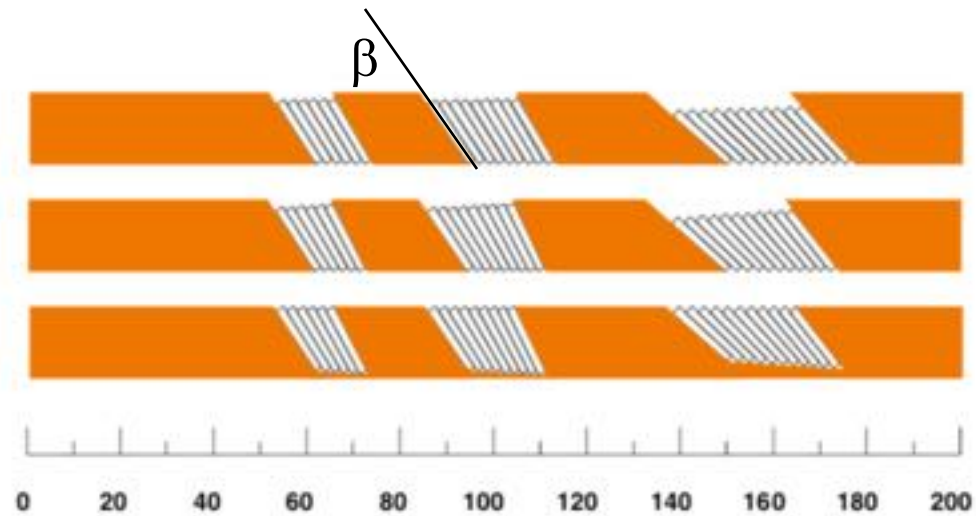
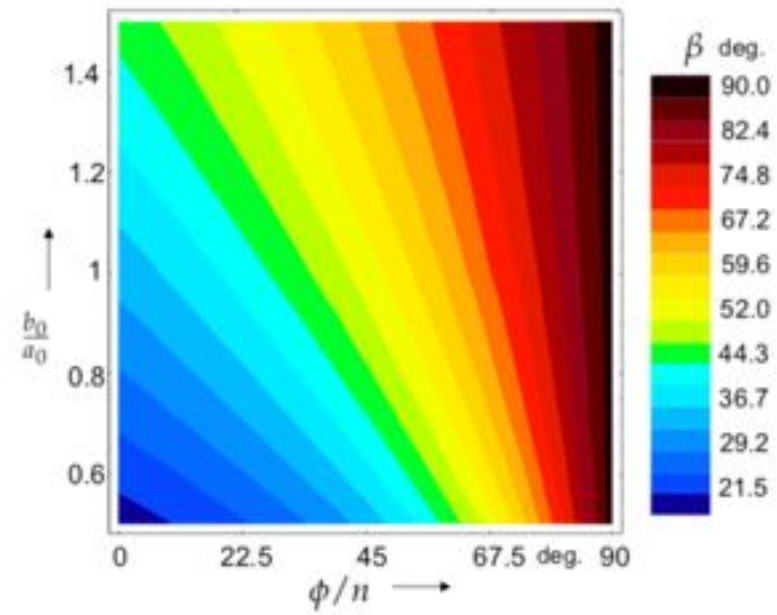
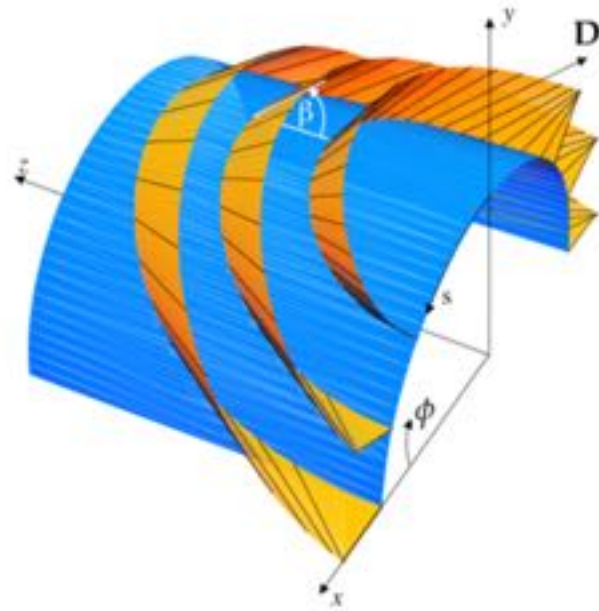
$$\mathbf{r}(t) = R \sin\left(\frac{a_a}{R} \cos^{\frac{2}{n}} t\right) \mathbf{e}_x + R \cos\left(\frac{a_a}{R} \cos^{\frac{2}{n}} t\right) \mathbf{e}_y + b_a \sin^{\frac{2}{n}} t \mathbf{e}_z$$

$$\mathbf{T}(t) = \frac{\mathbf{v}(t)}{|\mathbf{v}(t)|}, \quad \mathbf{B}(t) = \frac{\mathbf{v}(t) \times \mathbf{a}(t)}{|\mathbf{v}(t) \times \mathbf{a}(t)|}, \quad \mathbf{N}(t) = \frac{(\mathbf{v}(t) \times \mathbf{a}(t)) \times \mathbf{v}(t)}{|\mathbf{v}(t) \times \mathbf{a}(t)| |\mathbf{v}(t)|},$$

$$\kappa(t) = \frac{|\mathbf{v}(t) \times \mathbf{a}(t)|}{|\mathbf{v}(t)|^3}, \quad \tau(t) = \frac{(\mathbf{v}(t) \times \mathbf{a}(t)) \cdot \dot{\mathbf{a}}(t)}{|\mathbf{v}(t) \times \mathbf{a}(t)|^2}.$$

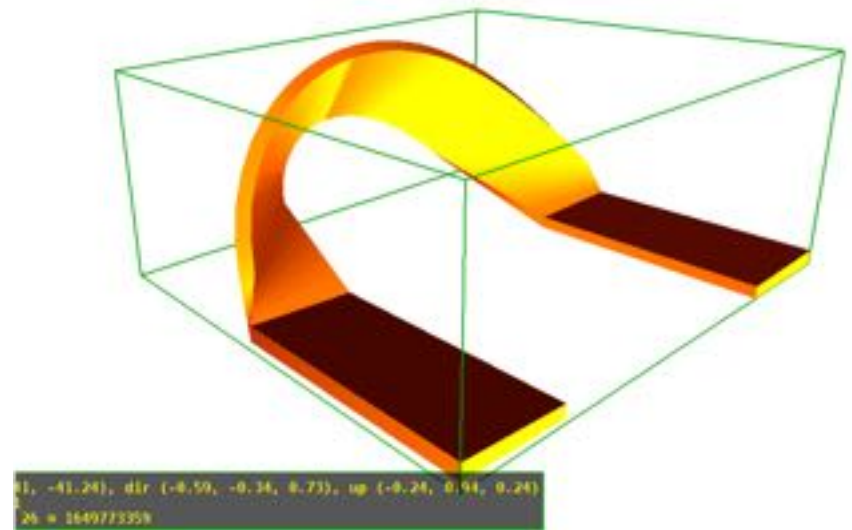
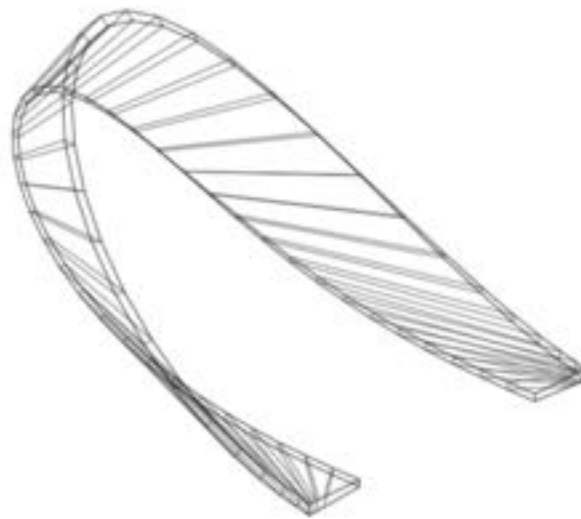
- The ellipticity of the base curve λ_e .
- The order n of the base curve.
- The inclination angle β between the innermost turn of each coil block.
- Four knots of a cubic spline function allowing for the local adjustment of the cable torsion between the onset of the coil end and the nose, ac-

The "Natural" Angle

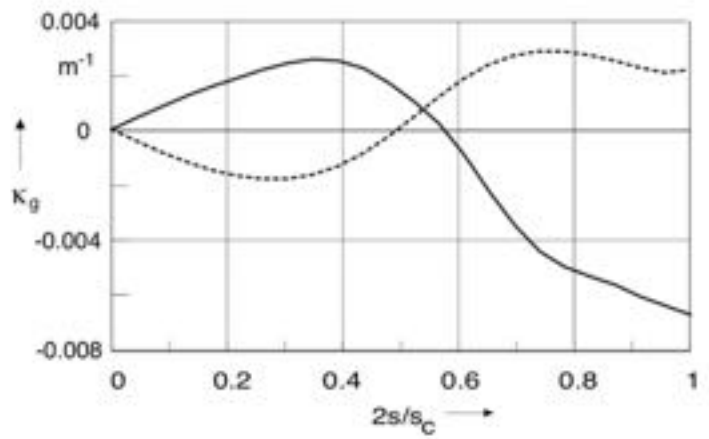
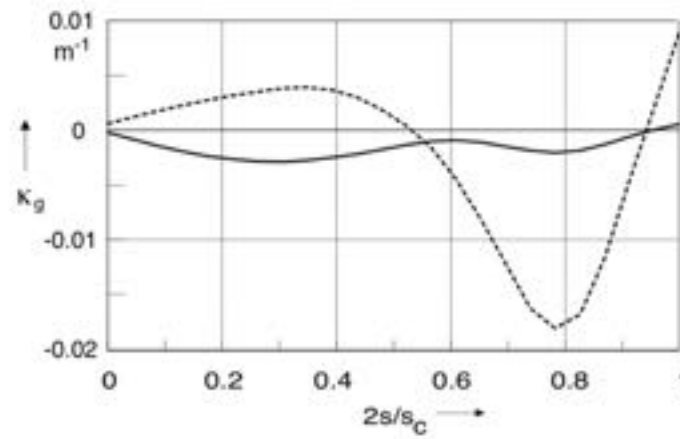
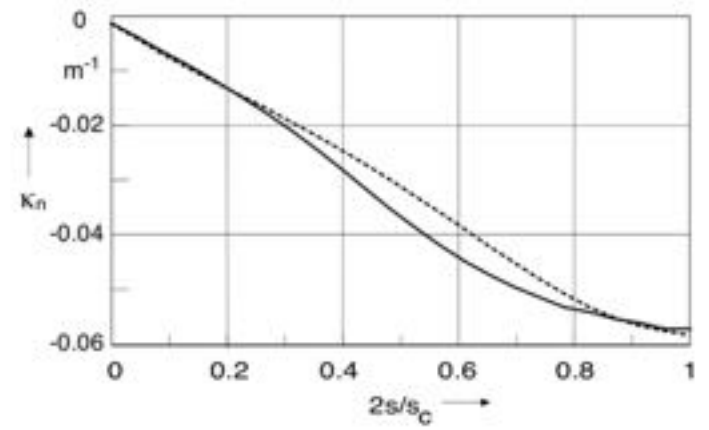
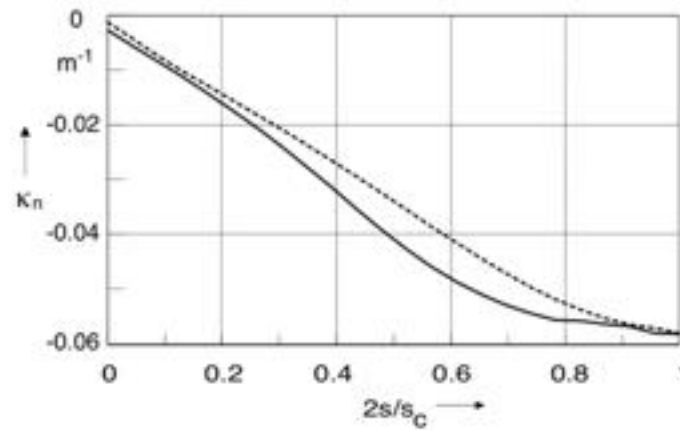


Objectives

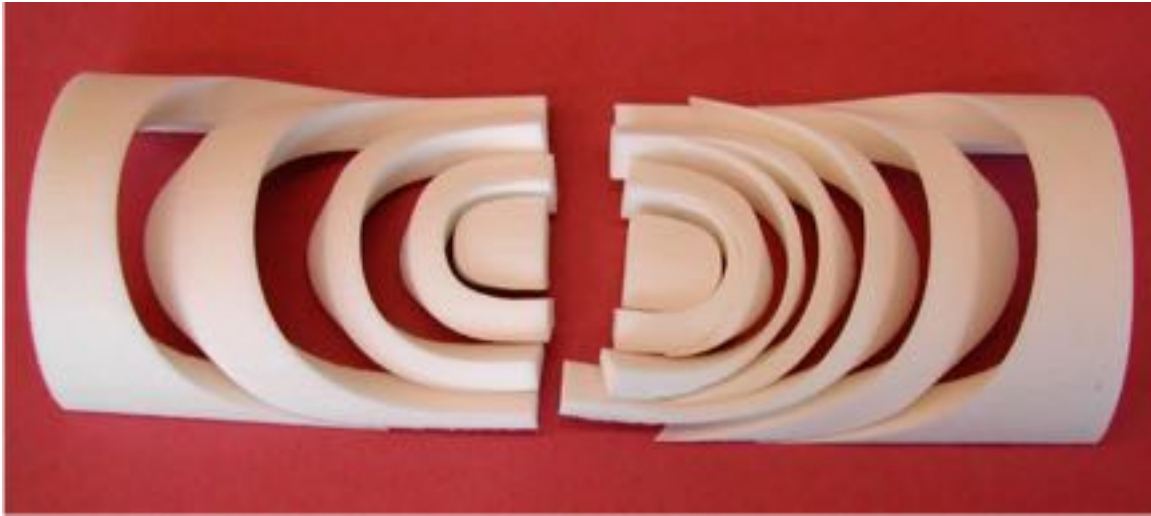
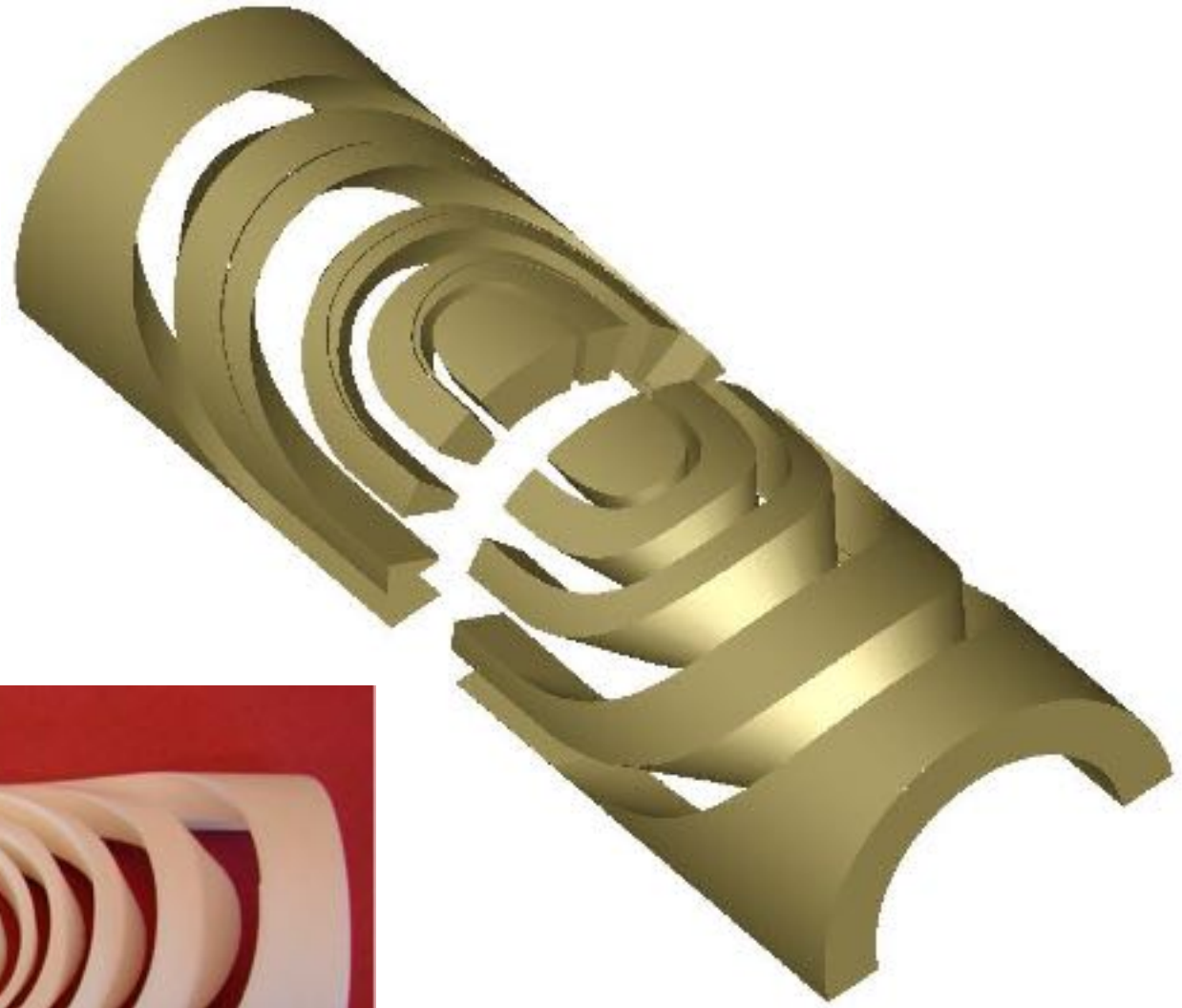
- Integrated squared geodesic curvature of each coil block.
- Maximum curvature parameters in each coil block.
- A parameter indicating an edge of regression violation within the strip surface.



Normal and Geodesic Curvature



End-spacer Prototyping



End-Spacer Prototyping



Sintering (Titanium)



Machining (Epoxy-Glass, G11)

Endspacer Machining



Winding Tests

